"Hydrogen Atom Transfers in B_{12} Enzymes," R. Banerjee, D. G. Truhlar, A. Dybala-Defratyka, P. Paneth, in *Hydrogen Transfer Reactions*, edited by J. T. Hynes, J. P. Klinman, H.-H. Limbach, and R. L. Schowen (Wiley-VCH, Weinheim, Germany, 2007), Vol. 4, pp. 1473-1495.

19
Hydrogen Atom Transfers in B_{12} Enzymes

Ruma Banerjee, Donald G. Truhlar, Agnieszka Dybala-Defratyka, and Piotr Paneth

19.1
Introduction to B_{12} Enzymes

B_{12} is a tetrapyrrolic-derived organometallic cofactor that supports three subfamilies of enzymes in microbes and in animals, the isomerases, the methyltransferases, and the dehalogenases [1]. The corrin ring system is more reduced than the porphyrin ring system, is heavily ornamented peripherally, and is distinguished by a central cobalt atom that is coordinated equatorially to four pyrrolic nitrogens. The cobalt can cycle between three oxidation states, +1 to +3, and the unique properties of each species are exploited in the chemistry of the reactions catalyzed by B_{12} enzymes. In both the methyltransferase and isomerase subfamilies of B_{12} enzymes, the upper axial ligand to cobalt is an alkyl group and the cobalt is formally in the +3 oxidation state. The alkyl group is methyl and deoxyadenosyl in methylcobalamin (MeCbl) and coenzyme B_{12} (AdoCbl), respectively. Their structures are shown in Scheme 19.1. Dichotomous pathways for cleaving the organometallic cobalt–carbon bond yield different products with different reactivities. In the methyltransferases, the cobalt–methyl bond ruptures heterolytically, and the products are cob(I)alamin (vitamin B_{12} with cobalt in the +1 oxidation state) and a carbocation equivalent that is transferred to a nucleophile. Cob(I)alamin is highly reactive and indeed, is regarded as nature's supernucleophile [2]. Its reactivity is exploited in biology for transferring methyl groups from unactivated methyl donors, viz. 5-methyltetrahydrofolate. In contrast, the cobalt–carbon bond is cleaved homolytically in the isomerases, where the upper axial ligand is a 5′-deoxyadenosyl group, and the coenzyme is called 5′-deoxyadenosyl cobalamin (AdoCbl). The radical products are cob(II)alamin (vitamin B_{12} with cobalt in the +2 oxidation state) and the reactive 5′-deoxyadenosyl radical, which is abbreviated dAdo•. The reactivity of the latter is harnessed to effect hydrogen atom abstractions in unusual and chemically challenging 1,2 rearrangement reactions involving the exchange of a variable group with a hydrogen atom on adjacent carbons.

Our understanding of the reaction mechanism of B_{12}-dependent reductive dehalogenations is quite limited [1]. However, the role of the cofactor appears to be sub-

Hydrogen-Transfer Reactions. Edited by J. T. Hynes, J. P. Klinman, H.-H. Limbach, and R. L. Schowen

ISBN: 978-3-527-30777-7

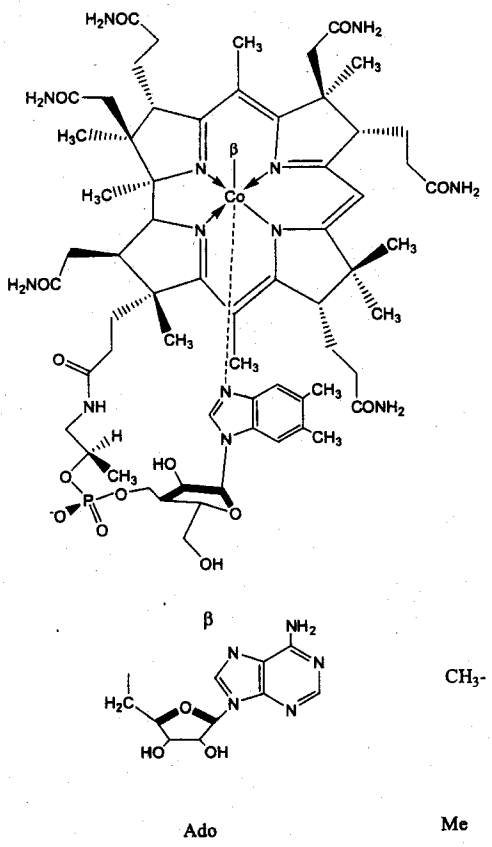

Scheme 19.1

stantially different from its role in the other two groups of B_{12}-dependent enzymes. It appears likely that the low redox potential of the Co(I) state of the cofactor is exploited to drive the reductive dehalogenation reactions.

The lower axial ligand in B_{12} derivatives is an extension of a peripheral propanolamine chain from ring D of the tetrapyrrolic structure. A variety of ligands are found in this position in nature, and the unusual base, 5,6-dimethylbenzimidazole, is the lower axial ligand in cobalamins. At acidic pH, the lower axial ligand is displaced via protonation. The cofactor can thus exist in two conformations, "base-on" and "base-off". However, the crystal structure of methionine synthase revealed yet another conformation, "base-off/His-on", in which the endogenous ligand is displaced and replaced by a histidine residue donated by the protein [3]. This ligand switch by an active site histidine embedded in a conserved DXHXXG motif [4] has since been observed in a number of other B_{12} enzymes including methylmalonyl-CoA mutase [5], glutamate mutase [6], and lysine amino mutase [7]. In contrast, a

second subclass of AdoCbl-dependent enzymes, including diol dehydratase [8] and ribonucleotide reductase [9], binds the cofactor in the "base-on" conformation.

19.2
Overall Reaction Mechanisms of Isomerases

Isomerases that are dependent on coenzyme B_{12} constitute the largest subfamily of B_{12} enzymes and are components of a number of fermentative pathways in microbes [10, 11]. A single member of this group of enzymes, methylmalonyl-CoA mutase, is found in both bacteria and in mammals where it is a mitochondrial enzyme involved in the catabolism of odd-chain fatty acids, branched chain amino

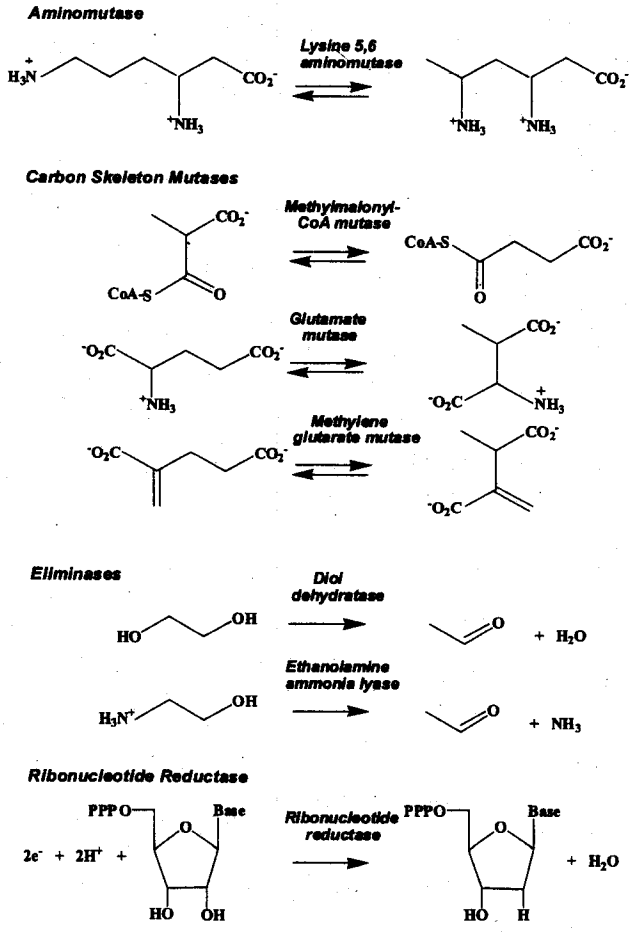

Scheme 19.2

acids, and cholesterol [12]. The general reaction catalyzed by the isomerases is a 1,2 interchange of a hydrogen atom and a variable group such as a group containing a heteroatom (hydroxyl or amino) or a carbon skeleton (see Scheme 19.2). One member, ribonucleotide reductase, uses the B_{12} cofactor to effect reductive elimination in the conversion of ribonucleotides to deoxyribonucleotides and represents a third class of this subfamily. As might be expected, individual enzymes differ somewhat in their radical generating strategies, as discussed below.

Whereas heterolytic cleavage in the methyltransferases is facilitated by methylcobalamin, homolytic cleavage is deployed by enzymes that resort to radical chemistry to effect difficult transformations. The preference for homolytic cleavage in AdoCbl may be related to the increased electron density on cobalt in the presence of the 5′-deoxyadenosyl group [13]. The chemical basis for the utility of the AdoCbl cofactor as a radical reservoir is the weak cobalt–carbon bond with a bond dissociation energy that is estimated to be ~30 kcal mol^{-1} (in aqueous solution) in the "base-on" state [14]. Reversible cleavage and reformation of the cobalt–carbon bond during catalytic turnover results in the formation of transient radical intermediates.

The first common step in AdoCbl-dependent reactions is homolytic cleavage of the cobalt–carbon bond to generate a radical pair, cob(II)alamin and the carbon-centered dAdo• radical (Scheme 19.3). This reaction experiences a ~10^{12}-fold rate enhancement in B_{12} enzymes [14, 15] in the presence of substrate, and the mechanism for this rate acceleration has been the subject of extensive scrutiny. Thus, in methylmalonyl-CoA mutase and in glutamate mutase, little if any destabilization of the cobalt–carbon bond is observed in the reactant state, as revealed by resonance Raman spectroscopy [16, 17], and the intrinsic substrate binding is utilized to labilize the bond. In contrast, approximately half of the destabilization of the cobalt–carbon bond in diol dehydratase is expressed in the reactant state. This re-

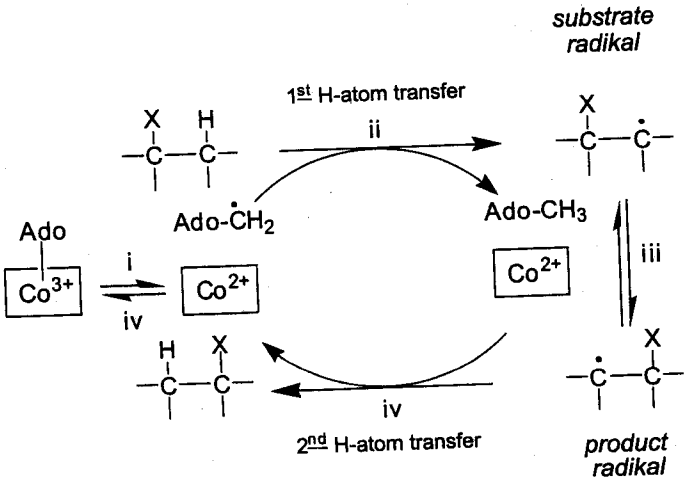

Scheme 19.3

actant destabilization may result in part from differences in the sizes of substrates that could translate into differences in binding energy. The destabilization renders the enzyme more prone to inactivation [10]; enzymes such as diol dehydratase can probably tolerate a higher inactivation rate due to the presence of repair chaperones that can catalyze the exchange of inactive cofactor for AdoCbl [18].

Rapid reaction studies on B_{12} enzymes reveal that homolysis is fast and not rate limiting [19–23]. Following homolysis, a series of controlled radical propagation steps result in migration of the organic radical (X in Scheme 19.3) to an adjacent carbon. The isomerization reaction is initiated by abstraction of a hydrogen atom from the substrate to generate a substrate-centered radical. This rearranges to a product-centered radical which reabstracts a 5′-hydrogen atom from 5′-deoxyadenosine. The dAdo• and cob(II)alamin radicals then recombine to complete a catalytic turnover cycle. In these 1,2 rearrangements, the hydrogen atom migrates intermolecularly, and a minimum of two hydrogen atom transfers, from substrate to dAdo• and back, are involved. A mechanistic complication may involve some competition of a 1,2-hydrogen shift along with the dominant 1,2 shift of the carbon-centered radical [24].

A key issue to understanding these reactions is ascertaining the role of the protein [25]. In bacterial methylmalonyl-CoA mutase, the substrate is bound inside an α/β barrel, which may be important for shielding the radical intermediates [5, 26, 27]. More significant catalytically may be the role of an active-site tyrosine [28, 29], which appears to sterically drive the adenosyl group off the Co, as a result of a conformational change upon substrate binding. EPR spectroscopy provides information about the distance of the dominant product radical from cob(II)alamin [30]. Finally, it is important to consider the role of entropy and the "solvating" power of the protein in promoting cobalt–carbon bond fission [31].

A critical issue for AdoCbl-dependent enzymes is controlling the timing of the homolysis step so that the radical pool is not dissipated. Homolysis of the cobalt–carbon bond takes place in the absence of substrate, as evidenced by the scrambling of label at the C5′ position in methylmalonyl-CoA mutase [32]. However, the equilibrium favors geminate recombination, and formation of the spectrally visible cob(II)alamin is not detected in the absence of substrate. Substrate binding triggers conformational adjustments, and the equilibrium shifts to favor the forward propagation of dAdo•. Thus, homolysis and hydrogen transfer from the substrate are kinetically coupled; evidence for this was first obtained with methylmalonyl-CoA mutase [20] and later with other enzymes, viz. glutamate mutase [33] and ethanolamine ammonia lyase [34]. In methylmalonyl-CoA mutase, substitution of the protons on the methyl group of methylmalonyl-CoA with deuterons decelerated the appearance of cob(II)alamin by ~20-fold at 25 °C [20]. This unusual sensitivity of the homolysis reaction of the cofactor to isotopic substitution in the substrate was interpreted as evidence for kinetic coupling, whereby the detectable accumulation of cob(II)alamin was dependent on the extent of H-atom abstraction from the substrate. Kinetic coupling effectively shifts the equilibrium of the homolysis reaction, and it allows the substrate to gate mobilization of radicals from the AdoCbl reservoir.

Ribonucleotide reductase presents an exception to the above mechanism where the working radical is a thiyl derived from an active-site cysteine (C408 in the *Lactobacillus leichmannii* enzyme) rather than dAdo• [35]. Mutation of C408 leads to failure of the mutant enzyme to generate detectable levels of cob(II)alamin. However, the mutant catalyzes epimerization of AdoCbl that is stereoselectively deuterated at the 5′ carbon bonded to cobalt [36]. This indicates that transient cleavage of the cobalt–carbon bond occurs, but when radical propagation to C408 is precluded, recombination of dAdo• and cob(II)alamin is favored.

19.3 Isotope Effects in B_{12} Enzymes

Large primary kinetic isotope effects have been measured for the H-atom transfer steps from substrate to dAdo• and from dAdo• to the product radical in a number of AdoCbl-dependent enzymes as indicated in Table 19.1. In methylmalonyl-CoA mutase, the steady-state deuterium isotope effect is 5-6 in the forward direction, and the intrinsic isotope effect of step (i) in Scheme 19.3 is masked by the kinetically coupled but slower later steps [37–39]. The steady-state tritium kinetic isotope effect (k_H/k_T) in the forward direction has been reported to be 3.2 [38]. Note that the experiments with deuterium were performed with a fully deuterated methyl group, while those with tritium were carried out at the trace level and correspond to a single isotopic atom; therefore these two isotope effects should not be directly compared. For the reverse reaction, the deuterium kinetic isotope effect is also par-

Table 19.1. Summary of kinetic isotope effects reported for B_{12}-dependent isomerases.

Enzyme *substrate*	Overall kinetic isotope effect		k_H/k_D on Co(II) formation	Ref.
	k_H/k_T	k_H/k_D		
Diol dehydratase				
propanediol	83 (10 °C)	10 (37 °C)	3–4 (4 °C)	10, 45
Ethanoloamine lyase (EAL)				
ethanolamine	107 (23 °C)	7.4 (23 °C)	>10 (22 °C)	34, 44
Methylmalonyl-CoA mutase (MCM)				
methylmalonyl-CoA	3.2 (~30 °C)	5–6 (30 °C)	43 (10 °C)	37–40
succinyl-CoA		3.4 (30 °C)		29
Glutamate mutase				
glutamate	21 (10 °C)	3.9 (10 °C)	28 (10 °C)	33, 43
3-methylaspartate	19 (10 °C)	6.3 (10 °C)	35 (10 °C)	33, 43

tially masked by kinetic complexity ($k_H/k_D = 3.4$) [38]. Under pre-steady-state conditions though, the measured kinetic isotope effects should not be affected by the product release step and, barring other complications, should be close to the intrinsic kinetic isotope effect. Under these conditions, a large deuterium isotope effect on cob(II)alamin formation has been reported for the conversion of methylmalonyl-CoA to succinyl-CoA [20, 40]. Since a protein-based hydrogen pool in methylmalonyl-CoA mutase, which could account for the anomalously large isotope effects, has been excluded [38], the involvement of tunneling was invoked [20]. An Arrhenius analysis of the temperature dependence of the pre-steady-state isotope effect has provided compelling evidence [40] that tunneling dominates the reaction in that the observed values of the ratio, A_H/A_D (0.078 ± 0.009), of pre-exponential factors and the difference, $E_{a,H} - E_{a,D}$ (3.41 ± 0.07 kcal mol^{-1}), of activation energies lie outside the ranges expected [41] ($A_H/A_D = 0.5$–1.4 and $E_{a,H} - E_{a,D}$ ca. <1.3 kcal mol^{-1}) in the absence of tunneling. The coupled homolysis/H-transfer steps catalyzed by methylmalonyl-CoA mutase are characterized by an equilibrium constant that is estimated to be close to unity and a phenomenological free energy of activation, $\Delta G^{\ddagger}$, of 13.1 ± 0.6 kcal mol^{-1} at 37 °C that corresponds to a $\sim 10^{12}$-fold [42] rate acceleration. In contrast, thermolysis of AdoCbl in solution is characterized by an unfavorable equilibrium, and a $\Delta G^{\ddagger}$ of 30 kcal mol^{-1} at 37 °C.

In glutamate mutase [43], the forward and reverse steady-state deuterium (k_H/k_D of 3.9 forward and 6.3 reverse) and tritium (k_H/k_T of 21 forward and 19 reverse) kinetic isotope effects are both suppressed. However large deuterium isotope effects of 28 and 35 in the forward and reverse directions respectively have been observed for cob(II)alamin formation under pre-steady-state conditions. These large kinetic isotope effects suggest that quantum mechanical tunneling also dominates this enzyme reaction.

Diol dehydratase and ethanolamine ammonia lyase exhibit the largest overall tritium isotope effects that have been measured in B_{12}-dependent enzymes [44, 45], the overall deuterium kinetic isotope effect is also substantial [10, 34, 45]. The observation of a deuterium isotope effect on the pre-steady-state formation of cob(II)alamin in diol dehyratase [10] and in ethanolamine ammonia lyase [25] is consistent with kinetic coupling between the homolysis and H-transfer steps.

Recently the secondary kinetic isotope effect has been measured for the Co–C homolysis step in the pre-steady-state reaction of glutamate mutase [46]. The result obtained was $k_H/k_T = 0.76 \pm 0.02$, which is a large inverse effect. The same study reported a secondary equilibrium isotope effect of $k_H/k_T = 0.72 \pm 0.04$. Thus the kinetic and equilibrium effects agree within the error bars, the most straightforward interpretation of which, in the absence of tunneling, would be that the dynamical bottleneck is close to the product, i.e., late. However in the light of the large role expected for tunneling, this conclusion is not justified. Tunneling would be expected to raise the secondary kinetic isotope effect, so the fact that the kinetic isotope effect is inverse seems very significant. Recall that the Co–C homolysis and the hydrogen transfer from substrate to dAdo•, though not likely to be concerted, are kinetically coupled. The homolysis step corresponds to a $sp^3 \rightarrow sp^2$ hybridiza-

tion change at C5′ and this direction of hybridization change usually makes a normal contribution to the secondary kinetic isotope effect [47], whereas the hydrogen transfer involves the opposite trend at C5′. Hence the net inverse kinetic isotope effect would seem to place the dynamical bottleneck of the kinetically coupled two-step process at the hydrogen transfer step.

19.4 Theoretical Approaches to Mechanisms of H-transfer in B_{12} Enzymes

It is not easy to infer the details of the hydrogen atom transfer steps from the experimental kinetics, and theoretical methods provide one possible way to increase understanding. Although computational approaches to the Co–C bond dissociation and radical rearrangement steps in B_{12}-dependent enzymes have been attempted [48–56], the hydrogen atom transfer has received less attention. The radical nature of the dAdo• reactant, the large size of the corrin moiety and the presence of a transition metal contribute to the difficulty of modeling this step in B_{12} enzymes. This difficulty is compounded by the paucity of reliable energetic data to calibrate the calculations. While good geometric information is sometimes sufficient for qualitative predictions of kinetic isotope effects for over the barrier processes, modeling the tunneling contribution [57–59] requires detailed knowledge of the ensemble of reaction paths, their barrier heights, the shapes (especially the widths) of the barriers, the curvature components of the reaction paths, and the potential energy in the tunneling swaths, which are the broad regions of configuration space through which tunneling from the reactant valleys to the product ones may proceed. Thus far only a few reports have been published on reactions that specifically aim at modeling the hydrogen atom transfer steps in B_{12}-dependent enzymes, and only one [60] addresses the tunneling contribution. Such calculations however are beginning to come within the realm of current computational technology, spurring new attempts at modeling H-atom transfer steps.

Several studies have addressed the energetics and geometry of H-atom transfer in reactions that serve as models for this step in B_{12}-dependent enzymes [61–65]. Although these studies do not include active site residues and do not attempt to address the non-classical behavior of this step, they do provide useful information. Since combined quantum mechanical/molecular mechanical (QM/MM) calculations [66] of the enzyme kinetics may require the inclusion of a large number of atoms in the QM part due to the size of the corrin moiety, it is advantageous to use an inexpensive quantum mechanical model such as semiempirical molecular orbital theory. Therefore, a study was carried out in which the performance of semiempirical methods was critically evaluated and compared to high-end theory levels for $C_nH_{2n+1} + C_nH_{2n+2}$ ($n = 1, 2, 3$) reactions [65]. Consensus values were evaluated from the high-level G3S//MP2(full)/6-31G(d), G3SX(MP3)//B3LYP/6-31G(2df,p), CBS-QB3//B3LYP/6-31G(d†), MCG3/3//MPW1K/6-31+G(d,p), MC-QCISD/3//MPW1K/6-31+G(d,p), MC-QCISD/3, MPW1K/MG3S, and MPW1K/MG3S//MPW1K/6-31+G(d,p) calculations. The energetics of the $n = 1$ species

Table 19.2. Calculated barrier heights (in kcal mol^{-1}) for $C_nH_{2n+1} + C_nH_{2n+2}$ ($n = 2, 3$) reactions[a]

Method	$C_2H_5^{\cdot} + C_2H_6$	$C_3H_7^{\cdot} + C_3H_8$
Consensus barrier height	16.7	16.0
AM1	16.0	15.6
PM3	12.0	12.5
AM1-CHC-SRP	18.3	17.9
PM3-CHC-SRP	17.0	16.3
PM3(tm)	16.3	15.6
B3LYP/6-31+G(d,p)[b]	15.7	15.5
MP2/6-31+G(d,p)[b]	19.4	18.6

[a] average values for *gauche* and *trans* structures. [b] The basis set is given after the solidus, using conventional notation [67].

($CH_3^{\cdot}$ and CH_4) differ significantly from that obtained for the larger models, indicating the inadequacy of a methyl species as a model for the larger molecules. Some key results [65] for $n = 2$ and 3 are shown in Table 19.2. This table shows that the general AM1 semiempirical parametrization [67] is capable of reproducing the barrier heights for transfer of a hydrogen atom between two carbons centers (the "CHC" motif) within ~1 kcal mol^{-1}, which is quite encouraging. The equally inexpensive PM3 parametrization [67] is much less accurate, but the PM3(tm) method [67] is about as accurate as AM1. Use of specific reaction parameters (SRP) [68] for CHC systems [65] also improves PM3, but is unable to systematically improve AM1. Table 19.2 also shows a more expensive semiempirical method, B3LYP [67], which is a hybrid of Hartree–Fock theory and density functional theory, and it shows an *ab initio* post-Hartree–Fock level, MP2 [67]. Although B3LYP usually underestimates barriers for hydrogen atom transfers [69], for the CHC motif the magnitude of the underestimate is not large, only 0.5–1.0 kcal mol^{-1} in Table 19.2.

Toraya et al. [60–63] used B3LYP (with the 6-311G(d) basis set) for calculations on the H-atom transfer steps in diol dehydratase reaction. Both H-atom transfers, i.e., from the substrate and re-abstraction of a hydrogen atom from 5′-deoxyadenosine, were considered. The models used in these studies included the substrate, 1,2-propanediol, a potassium cation found in the active site, and an ethyl radical as a mimic of the dAdo• radical (Fig. 19.1). The activation barrier for the abstraction of the *pro-S* hydrogen atom of substrate by dAdo• was calculated to be 9.0 kcal mol^{-1}, while the activation barrier for the reverse reaction between product radical and 5′-deoxyadenosine was 15.7 kcal mol^{-1}. In the absence of the potassium cation the forward activation barrier is 9.6 kcal mol^{-1} indicating that coordination of the substrate by the potassium cation has a minimal energetic effect on the H-atom transfer step, but seems to hold the substrate and intermediates in

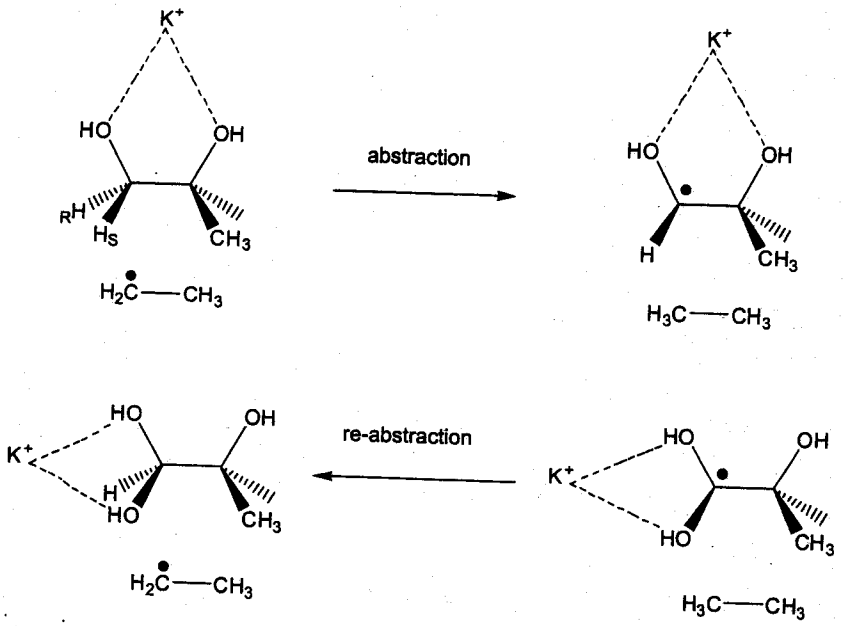

Figure 19.1. Model [61–63] of hydrogen atom transfer steps in diol dehydratase reaction.

position for the multistep sequence. These calculations disagree with the experimental [70] determination of the rate-determining step in that the barrier for hydrogen atom abstraction is lower than that for OH group migration, which is probably a consequence of omitting active-site residues, since calculations on other model systems show strong environmental effects on the OH migration [48, 49]. For the re-abstraction step, two pathways were considered that differ in the timing of dehydration (Fig. 19.1). When the dehydration step precedes the H-atom transfer step, an activation barrier of 19.8 kcal mol^{-1} is estimated. For the alternative pathway, in which hydrogen abstraction from deoxyadenosine by the product radical occurs prior to dehydration, the barrier is 15.1 kcal mol^{-1} and was proposed to be more likely. However, the lack of active site residues in this model precludes unequivocal exclusion of the first pathway.

The H-atom transfer steps in the reaction catalyzed by ethanolamine ammonia lyase reaction have also been examined computationally [64]. The simplest model employed a 1,5-dideoxyribose radical and 2-aminoethanol as the substrate (Fig. 19.2). The influence of full ($R^2 = H^+$) or partial protonation (R^2 = methyliminium = $NH_2CH_2^+$) of the nitrogen atom, as well as the synergetic presence of two ($R^1 = HCO_2^-$, R^2 = methyliminium = $NH_2CH_2^+$) hydrogen bonds, on the energetics of H-atom abstraction were evaluated. The hydrogen bonds mimic His and Asp residues in the active site, although the hydrogen bonds were arbitrarily placed since the 3D structure of the active site is not known. Two conformations of the ribose ring were considered. Calculations were carried out at B3LYP/6-

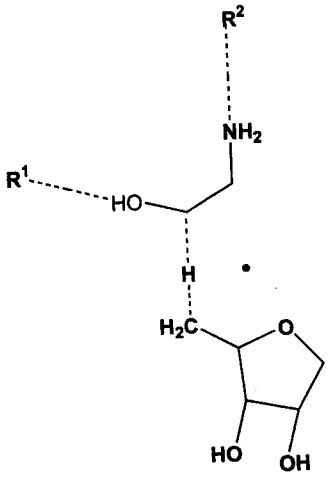

Figure 19.2. Model [64] of the hydrogen atom transfer between two CH_2 groups in ethanolamine ammonia lyase. See Section 19.4 of text for an explanation of R^1 and R^2.

311++G(d,p)//B3LYP/6-31G(d) and MP2/6-311++G(d,p)//B3LYP/6-31G(d) levels, and zero point vibrational energy was included. Activation enthalpies of 16.7 and 17.3 kcal mol^{-1} were found for the unprotonated substrate (R^1 and R^2 missing) and the ribose C3-*endo* and C2-*endo* conformers, respectively. The results indicate that the H-atom transfer step would be facilitated by protonation or by hydrogen bonding interactions to the substrate. In particular, activation enthalpies for models of fully protonated or singly hydrogen-bonded substrate were smaller than 15 kcal mol^{-1}, while the simultaneous presence of two hydrogen bonds to the nitrogen atom increased the activation barrier to over 25 kcal mol^{-1}.

Finally we consider some attempts to simulate the tunneling contributions in the hydrogen transfer step. This was first attempted using several models of differing complexity [60, 71]. PM3 calculations using conventional transition state theory (TST) [72] and a model comprising 37 atoms of the ribose radical and methylmalonyl with truncated CoA moiety (Fig. 19.3 with $R^3 = H$ and R^4 missing) give a hydrogen kinetic isotope effect (for CH_3 vs. CD_3) of only about 10, indicating that TST without tunneling corrections is insufficient to account for the experimental results, which are summarized in column 2 of Table 19.4. To include tunneling, the barrier shape was estimated from the energies of three stationary points (the substrate, the transition state, and the product of the hydrogen atom reaction) by an algorithm called IVTST-0 that was developed earlier [73] for gas-phase reactions. This treatment allows the calculation of a multidimensional tunneling contribution. The resulting dynamical method [74, 75] is called TST/ZCT (where ZCT denotes zero-curvature tunneling, since this method ignores the curvature of the reaction path, which is discussed below). Calculated energetics (Table 19.3, column 3) and kinetic isotope effects (Table 19.4, column 4) compare reason-

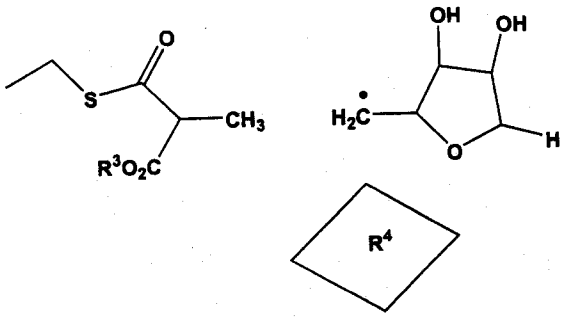

Figure 19.3. Models [60] used in calculations of hydrogen kinetic isotope effects with tunneling contributions.

Table 19.3. Classical barrier heights and energies of reaction (in kcal mol^{-1}) for models[a] of the hydrogen abstraction for methylmalonyl-CoA mutase.

	QM	PM3	M[b]	PM3	PM3(tm)	PM3(tm)	PM3
	R^3	H	H	Arg	H	Arg	...
	R^4	...	...	...	...	Corrin+His	...
Ref.		60	71	60	71	60	60
barrier height[c]		11.9	14.4	12.0	16.2	19.9	4.5
reaction energy[d]		−0.2	0.7	−0.6	−0.1	9.5	−2.6

[a] R^3 and R^4 are explained in Fig. 19.3. [b] M denotes MPW1K/6-31+G(d,p). [c] The change in potential energy (exclusive of zero-point energy) in proceeding from reactants to the saddle point. [d] The change in potential energy (exclusive of zero-point energy) in proceeding from reactants to products.

Table 19.4. Primary kinetic isotope effects for hydrogen abstraction from methylmalonyl-CoA.

T (°C)	Exp.	QM	PM3	M[a]	PM3	PM3(tm)	PM3(tm)	PM3
		R^3	H	H	Arg	H	Arg	...
		R^4	...	...	...	...	Corrin+His	...
Ref.	40		60	71	60	71	60	60
5	50		47	42	49	118	63	9.4
20	36		37	32	38	84	49	8.6

[a] M denotes MPW1K/6-31+G(d,p).

ably well with results carried out at the MPW1K/6-31+G(d,p) level (Table 19.3, column 4 and Table 19.4, column 5), which has been validated to give reliable results for hydrogen atom transfer reactions [69]. Inclusion of arginine, which is hydrogen-bonded to the carboxylate of the methylmalonyl moiety in the crystal structure, does not affect the results very much (Table 19.3 column 5 and Table 19.4, column 6).

However, the agreement between these results and the experimental values is only coincidental. When the PM3tm method, which gives a higher barrier height is used (Table 19.3, column 6), the TST/ZCT hydrogen kinetic isotope effect is much higher (Table 19.4, column 7). Further enlargement of the model to include the corrin moiety with an imidazole ring (Table 19.3, column 7 and Table 19.4, column 8) does not change the isotope effect very much, but deprotonation of the carboxyl group leads to substantial lowering of the barrier (Table 19.3, column 8) and consequently, a much smaller kinetic isotope effect (Table 19.4, column 9), illustrating the sensitivity of the calculated isotope effect to the barrier height.

As the next step in improving the dynamical description, it is important to include reaction path curvature (as well as zero point variation) in the description of the tunneling event. If the minimum energy path (MEP) from reactants to products were a straight line in the space of atomic Cartesian coordinates, there would be no internal centrifugal effect (bobsled effect) forcing the system's motion, on average, to deviate from the MEP. But the MEP for most reactions is curved, and there is a bobsled effect. For tunneling processes the bobsled effect is negative (because the semiclassical kinetic energy is negative) [76–78] and thus the dominant tunneling paths are on the concave side of the MEP. This phenomenon is called corner-cutting tunneling [78, 79].

To describe the tunneling process in more detail, we need to define some terminology. A transition state (or generalized transition state) is a dividing surface (technically a hypersurface) in phase space (the space of the nuclear coordinates and momenta); here we define transition states entirely in terms of their location in coordinate space, which, after separating translation and rotational motion, has $3N - 6$ dimensions, where N is the number of atoms; and we consider transition states that are orthogonal to the MEP. Distance along the MEP is the reaction coordinate. Because the reaction coordinate has a fixed value in a transition state, a transition state has $3N - 7$ vibrations, which are called its generalized normal modes (the word "generalized" is included because conventional normal modes are defined only at stationary points such as equilibrium geometries and saddle points). The conventional transition state passes through the saddle point, but generalized transition states intersect the MEP both earlier and later than the saddle point.

Reaction path curvature is actually a vector with $3N - 7$ components [80]. Each component is associated with a particular generalized normal mode, and it measures the extent to which the system curves into a particular direction as it progresses along the MEP. Corner-cutting tunneling involves a coupled motion involving the reaction coordinate and all the generalized normal modes that are associated with nonzero curvature components [81].

When reaction-path curvature is small, the tunneling is dominated by paths on

the concave side of the MEP whose locations are determined by the reaction-path curvature components [81, 82]. These small-curvature tunneling paths are typically located close enough to the MEP that the harmonic approximation is valid, and thus the dominant tunneling paths may be calculated (approximately) from the $3N-7$ curvature components and the $3N-7$ harmonic force constants of the generalized normal modes. From this information and the shape of the potential energy along the MEP, one can then calculate the tunneling probabilities. This is called the small-curvature tunneling (SCT) approximation [82, 83].

Describing tunneling in terms of definite paths in coordinate space [84] is a classical-like approximation. This kind of approximation (like the well known WKB method [85]) is called "semiclassical" in chemical physics (and here) because it involves calculating a quantum mechanical quantity by classical-like methods; thus it is partly classical or semiclassical. Unfortunately the kinetic isotope effect community uses the word "semiclassical" to denote an entirely different approximation, namely including quantized vibrational energies in the treatment of the $3N-7$ transition state vibrations, but treating the transmission coefficient entirely classically and thus completely neglecting tunneling. (This is sometimes called "quasiclassical" in chemical physics.) We hope this warning is sufficient to prevent confusion.

When reaction-path curvature is large, one requires a much more complicated semiclassical treatment to handle the tunneling. In the limit of large reaction-path curvature, tunneling tends to occur along straight-line tunneling paths because the shortest distance between two points is a straight line, and when reaction-path curvature is large, tunneling along short tunneling paths has a greatly enhanced probability [86]. In addition, tunneling tends to be much more delocalized, and systems may have appreciable probability of tunneling directly into vibrationally excited stretching modes [86, 87, 89]. A semiclassical theory that incorporates all of these features has been developed [82, 90, 91] and it is called the large-curvature tunneling (LCT) approximation.

In the general case one could obtain a good semiclassical tunneling approximation by optimizing the tunneling path somewhere between the small-curvature and large-curvature limits by a least-action approximation [92]. In practice, it has been found that simply choosing between the SCT and LCT approximations on the basis of whichever yields a larger tunneling probability (the tunneling is dominated by the most favorable tunneling paths at each tunneling energy) is enough optimization to yield accurate results [91, 93]. This is called microcanonically optimized multidimensional tunneling or μOMT [91, 93].

Tunneling can be included most consistently in transition state theory in the context of variational transition state theory, e.g., canonical variational theory (CVT) [75]. CVT calculations were performed [71] with zero-curvature tunneling (see Table 19.5, column 3), and they show that the IVTST-0 calculations overestimate ZCT contribution to the hydrogen kinetic isotope effect. Calculations were also performed including corner-cutting tunneling, and these are shown in the last five columns of Table 19.5. As can be seen from the comparison of the results in these columns, large-curvature tunneling (LCT) plays the dominant role. Col-

Table 19.5. Kinetic isotope effects for 37-atom model obtained using PM3 for electronic structure calculations.

T (°C)	CVT[a]	CVT/ZCT	CVT/SCT	CVT/LCT	CVT/μOMT		
QM model	PM3 M37[b]	PM3 M37	PM3 M37	PM3 M37	PM3 M37	PM3 M50[c]	AM1 M37
5	9.9	21	27	145	113	96	127
20	8.5	18	23	124	94	80	89

[a] No tunneling. [b] 37-atom model corresponding to $R^3 = H$, and R^4 not present. [c] 50-atom model: M37 + adenine.

umns 6 and 7 of Table 19.5 show that comparable results are obtained when the model is enlarged to include adenine, the last column contains results obtained for the AM1 Hamiltonian instead of PM3. Barriers for the AM1 parameterizations are 14.9 and 16.6 kcal mol^{-1} for the M37 and M50 models, respectively.

The last three columns of Table 19.5 report results obtained with the microcanonically optimized multidimensional tunneling approximation, which represents the currently most trusted method for including a tunneling contribution. These results predict that the hydrogen kinetic isotope effect for the hydrogen atom step in methylmalonyl-CoA reaction in the direction of succinyl formation is ~100.

The dynamical calculations in Tables 19.4 and 19.5 were performed with the POLYRATE [88] and MORATE [90] computer programs.

19.5 Free Energy Profile for Cobalt–Carbon Bond Cleavage and H-atom Transfer Steps

The interpretation of kinetic isotope effects observed in enzymes must take account of kinetic complexity. For example, the deuterium kinetic isotope effect on the methylmalonyl-CoA mutase-catalyzed reaction was measured under pre-steady-state conditions with UV–visible detection of cob(II)alamin formation [20, 42]. Thus, it reports on a combination of steps, including substrate binding and a concomitant conformational change in the enzyme, cobalt-carbon bond homolysis, and hydrogen-atom transfer to the dAdo• radical. The kinetics could be further complicated in other enzymes such as diol dehydratase [95] and glutamate mutase [96], where conformational changes in the dAdo• radical are expected to occur between the homolysis and hydrogen atom transfer steps, and in ribonucleoside triphosphate reductase, in which a protein-based cysteinyl radical functions as the working radical [97]. Because of these mechanistic complexities, observed kinetic isotope effects under pre-steady state conditions, although large, need not reflect

the full intrinsic values for the kinetic isotope effects on the H-atom transfer steps in the respective enzymes. Thus it is unclear whether the difference between the large intrinsic kinetic isotope effect calculated for the hydrogen atom transfer step in methylmalonyl-CoA mutase and the isotope effect observed experimentally (which is also very large, but not as large as the calculated one) indicates that kinetic complexity causes about half of the isotope effect to be masked by isotope-insensitive steps in the observed pre-steady-state rate or whether it results from the quantitative uncertainty of the calculation. Since the calculation includes neither the full enzyme nor ensemble averaging, one should be very cautious about the former type of conclusion.

Further progress toward a quantitative resolution of the size of the intrinsic kinetic isotope effect requires a more complete mechanistic analysis, which is sometimes [98], but not always, possible. A step in this direction has been made for methylmalonyl-CoA mutase [42], for which a free energy profile extending across seven steps has been constructed on the basis of available kinetic and spectroscopic data. Similarly, a three-step profile has been presented for ethanolamine deaminase [99], and a six-step profile has been presented for glutamate mutase [22]. A feature seen in the profiles of both methylmalonyl-CoA mutase and glutamate mutase, which is also seen for many other enzymes, is that the energetic barriers to the interconversion of the various chemical intermediates are similar in height, which may be a general consequence of the tendency of enzymatic transformations to be partitioned into a series of discrete steps without the inefficiency of high energy release or high energy consumption in any one of them. In any event, it is precisely this feature that makes it hard to sort out elementary-step rate constants and kinetic isotope effects for the individual chemical steps.

19.6 Model Reactions

We discussed above some theoretical studies of model systems. There is an even larger literature devoted to experimental studies of model systems, dating back at least 20 years [100, 101]. Most recently, some model studies have appeared that are directly related to the present concerns. In particular, Finke and coworkers [102, 103] have studied the reaction of β-neopentyl-Cbl with ethylene glycol (a model of the diol dehydratase reaction) at temperatures up to 120 °C, and their results have engendered interesting discussions [104]. Their key finding is that the elevated-temperature kinetic isotope effects observed for the model reaction in solution (where the enzyme is not present to stabilize the dAdo• radical) are very similar to those obtained for methylmalonyl–CoA mutase at temperatures more typical of physiological action. The comparison is clouded by potential kinetic complexity, discussed above, that may suppress the intrinsic value of the kinetic isotope effect in the enzyme case. Nevertheless one clear conclusion of this work, which agrees with pure theoretical considerations as well as with studies of many nonenzymatic reactions, is that enzymes are not uniquely evolved to promote tunneling. Whether

the fraction of a reaction that proceeds by tunneling in an enzyme reaction is greater than that in a similar nonenzymatic reaction will depend on the individual enzyme and on many detailed mechanistic factors. One scenario is that the environment can exert a greater leverage on a reaction by lowering the effective barrier height (which appears in an exponent) than by changing the transmission coefficient, and lower barriers are often (not always) associated with broader barrier tops; a lower, broader barrier makes it harder for tunneling to compete with over-barrier processes so that the fraction of reactive events that occurs by tunneling may be lower in the enzymatic system. If the intrinsic methylmalonyl–CoA mutase kinetic isotope effect is as large as the calculated values given above, though, then this reaction may prove to be an exception to that scenario.

19.7 Summary

Deconvoluting the contributions of the individual steps in the observed pre-steady-state rate constant for cob(II)alamin formation is challenging and awaits solution. In particular, details of the H-atom transfer steps elude direct determination. However, recent advances in the theoretical methodology hold promise for complementing the experimental analysis of a fundamental aspect of AdoCbl-dependent reactions, i.e., the H-atom transfer steps.

Acknowledgments

This work was supported by grants from the National Institutes of Health (Fogarty International Collaboration grant to P.P. and R.B. and DK45776 to R.B.) and the National Science Foundation (CHE-0349122 to D.T.).

References

1 Banerjee, R., Ragsdale, S. W. (2003) The many faces of vitamin B_{12}: Catalysis by cobalamin-dependent enzymes, *Annu. Rev. Biochem. 72*, 209–247.

2 Schrauzer, G. N., Deutsch, E. (1969) Reactions of cobalt(I) supernucleophiles. The alkylation of vitamin B_{12s}, cobaloximes(I), and related compounds, *J. Am. Chem. Soc. 91*, 3341–3350.

3 Drennan, C. L., Huang, S., Drummond, J. T., Matthews, R., Ludwig, M. L. (1994) How a protein binds B_{12}: A 3 Å X-ray structure of B_{12}-binding domains of methionine synthase, *Science 266*, 1669–1674.

4 Marsh, E. N. G., Holloway, D. E. (1992) Cloning and sequencing of glutamate mutase component S from *Clostridium tetanomorphum*, *FEBS Lett. 310*, 167–170.

5 Mancia, F., Keep, N. H., Nakagawa, A., Leadlay, P. F., McSweeney, S., Rasmussen, B., Bösecke, P., Diat, O., Evans, P. R. (1996) How coenzyme B_{12} radicals are generated: The crystal structure of methylmalonyl-coenzyme A mutase at 2 Å resolution, *Structure 4*, 339–350.

6 Reitzer, R., Gruber, K., Jogl, G., Wagner, U. G., Bothe, H., Buckel, W., Kratky, C. (1999) Glutamate mutase from Clostridium cochlearium: the structure of a coenzyme B_{12}-dependent enzyme provides new mechanistic insights, *Structure Fold. Des. 7*, 891–902.

7 Chang, C. H., Frey, P. A. (2000) Cloning, sequencing, heterologous expression, purification, and characterization of adenosylcobalamin-dependent D-lysine 5,6-aminomutase from Clostridium sticklandii, *J. Biol. Chem. 275*, 106–114.

8 Shibata, N., Masuda, J., Tobimatsu, T., Toraya, T., Suto, K., Morimoto, Y., Yasuoka, N. (1999) A new mode of B_{12} binding and the direct participation of a potassium ion in enzyme catalysis: X-ray structure of diol dehydratase, *Structure Fold Des. 7*, 997–1008.

9 Sintchak, M. D., Arjara, G., Kellogg, B. A., Stubbe, J., Drennan, C. L. (2002) The crystal structure of class II ribonucleotide reductase reveals how an allosterically regulated monomer mimics a dimer, *Nat. Struct. Biol. 9*, 293–300.

10 Toraya, T. (2003) Radical catalysis in coenzyme B_{12}-dependent isomerization (eliminating) reactions, *Chem. Rev. 103*, 2095–2127.

11 Banerjee, R. (2003) Radical carbon skeleton rearrangements: catalysis by coenzyme B_{12}-dependent mutases, *Chem. Rev. 103*, 2083–94.

12 Banerjee, R., Chowdhury, S. (1999) *Methylmalonyl-CoA Mutase*, John Wiley and Sons, New York.

13 Jensen, K. P., Sauer, S. P., Liljefors, T., Norrby, P.-O. (2001) Theoretical investigation of steric and electronic effects in coenzyme B_{12} models, *Organometallics 20*, 550–556.

14 Finke, R. G., Hay, B. P. (1984) Thermolysis of adenosylcobalamin: A product, kinetic and Co-C5′ bond dissociation energy study, *Inorg. Chem. 23*, 3041–3043.

15 Halpern, J. (1985) Mechanisms of coenzyme B_{12}-dependent rearrangements, *Science 227*, 869–875.

16 Dong, S., Padmakumar, R., Maiti, N., Banerjee, R., Spiro, T. G. (1998) Resonance Raman spectra of methylmalonyl-Coenzyme A mutase, a coenzyme B_{12}-dependent enzyme, reveal dramatic change in corrin ring conformation but little change in Co-C bond force constant in the cofactor upon its binding to the enzyme, *J. Am. Chem. Soc. 120*, 9947–9948.

17 Huhta, M. S., Chen, H. P., Hemann, C., Hille, C. R., Marsh, E. N. (2001) Protein-coenzyme interactions in adenosylcobalamin-dependent glutamate mutase, *Biochem. J. 355*, 131–137.

18 Mori, K., Toraya, T. (1999) Mechanism of reactivation of coenzyme B_{12}-dependent diol dehydratase by a molecular chaperone-like reactivating factor, *Biochemistry 38*, 13170–13178.

19 Hollaway, M. R., White, H. A., Joblin, K. N., Johnson, A. W., Lappert, M. F., Wallis, O. C. (1978) A spectrophotometric rapid kinetic study of reactions catalyzed by coenzyme B_{12}-dependent ethanolamine ammonia lyase, *Eur. J. Biochem. 82*, 143–154.

20 Padmakumar, R., Padmakumar, R., Banerjee, R. (1997) Evidence that cobalt-carbon bond homolysis is coupled to hydrogen atom abstraction from substrate in methylmalonyl-CoA mutase, *Biochemistry 36*, 3713–3718.

21 Brown, K. L., Li, J. (1998) Activation parameters for the carbon-cobalt bond homolysis of coenzyme B_{12} induced by the B_{12}-dependent ribonucleotide reductase from *Lactobacillus leichmannii*, *J. Am. Chem. Soc. 120*, 9466–9474.

22 Chih, H. W., Marsh, E. N. (1999) Pre-steady-state kinetic investigation of intermediates in the reaction catalyzed by adenosylcobalamin-dependent glutamate mutase, *Biochemistry 38*, 13684–13691.

23 Licht, S. S., Lawrence, C. C., Stubbe, J. (1999) Thermodynamic and kinetic studies on carbon-cobalt bond homolysis by ribonucleoside triphosphate reductase: the importance of

entropy in catalysis, *Biochemistry 38*, 1234–1242.

24 KUNZ, M., RÉTEY, J. (2000) Evidence for a 1,2 shift of a hydrogen atom in a radical intermediate of the methylmalonyl-CoA mutase reaction, *Bioorg. Chem. 28*, 134–139.

25 GARCIA-VILOCA, M., GAO, J., KARPLUS, M., TRUHLAR, D. G. (2004) How enzymes work: Analysis by modern rate theory and computer simulations, *Science 303*, 186–195.

26 BRANDEN, C., TOOZE, J. *Introduction to Protein Structure*, 2nd edn., Garland Publishing, New York, 1999, pp. 50–51.

27 THOMÄ, N. H., EVANS, P. R., LEADLAY, P. F. (2000) Protection of radical intermediates at the active site of adenosylcobalamin-dependent methylmalonyl-CoA mutase, *Biochemistry 39*, 9213–9221.

28 MANCIA, F., SMITH, G. A., EVANS, P. R. (1999) Crystal structure of substrate complexes of methylmalonyl-CoA mutase, *Biochemistry 38*, 7999–8005.

29 THOMÄ, N. H., MEIER, T. W., EVANS, P. R., LEADLAY, P. F. (1998) Stabilization of radical intermediates by an active site tyrosine residue in methylmalonyl-CoA mutase, *Biochemistry 37*, 14386–14393.

30 REED, G. H., MANSOORABADI, S. O. (2003) The positions of radical intermediates in the active sites of adenosylcobalamin-dependent enzymes, *Curr. Opin. Struct. Biol. 13*, 716–721.

31 PRATT, J. M. Cobalt in vitamin B_{12} and its enzymes, in *Handbook on Metalloproteins*, I. BERTINI, A. SIGEL, H. SIGEL (Eds.), Dekker, New York, 2001, pp. 603–668.

32 GAUDEMER, A., ZYBLER, J., ZYBLER, N., BARAN-MARSZAC, M., HULL, W. E., FOUNTOULAKIS, M., KONIG, A., WOLFE, K., RETEY, J. (1981) Reversible cleavage of the cobalt-carbon bond of coenzyme B_{12} catalyzed by methylmalonyl-CoA mutase from *Propionibacterium shermanii*: The use of coenzyme B_{12} stereospecifically deuterated in position 5′, *Eur. J. Biochem. 119*, 279–285.

33 MARSH, E. N. G., BALLOU, D. P. (1998) Coupling of cobalt-carbon bond homolysis and hydrogen atom abstraction in adenosylcobalamin-dependent glutamate mutase, *Biochemistry 37*, 11864–11872.

34 BANDARIAN, V., REED, G. H. (2000) Isotope effects in the transient phases of the reaction catalyzed by ethanolamine ammonia-lyase: determination of the number of exchangeable hydrogens in the enzyme-cofactor complex, *Biochemistry 39*, 12069–12075.

35 LICHT, S. S., BOOKER, S., STUBBE, J. (1999) Studies on the catalysis of carbon-cobalt bond homolysis by ribonucleoside triphosphate reductase: Evidence for concerted carbon-cobalt bond homolysis and thiyl radical formation, *Biochemistry 38*, 1221–1233.

36 CHEN, D., ABEND, A., STUBBE, J., FREY, P. A. (2003) Epimerization at carbon-5′ of (5′R)-[5′-^{2}H]adenosylcobalamin by ribonucleoside triphosphate reductase: Cysteine 408-independent cleavage of the Co-C5′ bond, *Biochemistry 42*, 4578–4584.

37 MICHENFELDER, M., HULL, W. E., RETEY, J. (1987) Quantitative measurement of the error in the cryptic stereospecificity of methylmalonyl-CoA mutase, *Eur. J. Biochem. 168*, 659–667.

38 MEIER, T. W., THOMÄ, N. H., LEADLAY, P. F. (1996) Tritium isotope effects in adenosylcobalamin-dependent methylmalonyl-CoA mutase, *Biochemistry 35*, 11791–11796.

39 CHOWDHURY, S., THOMAS, M. G., ESCALANTE-SEMERENA, J. C., BANERJEE, R. (2001) The coenzyme B_{12} analog 5′-Deoxyadenosylcobinamide-GDP supports catalysis by methylmalonyl-CoA mutase in the absence of trans-ligand coordination, *J. Biol. Chem. 276*, 1015–1019.

40 CHOWDHURY, S., BANERJEE, R. (2000) Evidence for quantum mechanical tunneling in the coupled cobalt carbon bond homolysis-substrate radical generation reaction catalyzed by methylmalonyl-CoA mutase, *J. Am. Chem. Soc. 122*, 5417–5418.

41 Saunders, W. H. Jr. Kinetic isotope effects, in *Investigation of Rates and Mechanisms of Reactions, Part I*, 4th edn., C. F. Bernasconi (Ed.), Wiley, New York, 1986, pp. 565–611.
42 Chowdhury, S., Banerjee, R. (2000) Thermodynamic and kinetic characterization of Co-C bond homolysis catalyzed by coenzyme B_{12}-dependent methylmalonyl-CoA mutase, *Biochemistry 39*, 7998–8006.
43 Chih, H. W., Marsh, E. N. (2001) Tritium partitioning and isotope effects in adenosylcobalamin-dependent glutamate mutase, *Biochemistry 40*, 13060–13067.
44 Weisblat, D. A., Babior, B. M. (1971) The mechanism of action of ethanolamine ammonia-lyase, a B_{12}-dependent enzyme. VIII. Further studies with compounds labeled with isotopes of hydrogen: Identification and some properties of the rate-limiting step, *J. Biol. Chem. 246*, 6064–6061.
45 Essenberg, M. K., Frey, P. A., Abeles, R. H. (1971) Studies on the mechanism of hydrogen transfer in the coenzyme B_{12} dependent dioldehydrase reaction II, *J. Am. Chem. Soc. 93*, 1242–1251.
46 Cheng, M. C., Marsh, E. N. G. (2004) Pre-steady-state measurement of intrinsic secondary tritium isotope effects associated with the homolysis of adenosylbcobalamin and the formation of 5′-deoxyadenosine in glutamate mutase, *Biochemistry 43*, 2155–2158.
47 Saunders, W. H. Jr., p. 598 of Ref 41.
48 Smith, D. M., Golding, B. T., Radom, L. (1999) Understanding the mechanism of B_{12}-dependent methylmalonyl-CoA mutase: Partial proton transfer in action, *J. Am. Chem. Soc. 121*, 9388–9399.
49 Smith, D. M., Golding, B. T., Radom, L. (2001) Understanding the mechanism of B_{12}-dependent diol dehydratase: a synergistic retro-push-pull proposal, *J. Am. Chem. Soc. 123*, 1664–1675.
50 Andruniow, T., Zgierski, M. Z., Kozlowski, P. M. (2001) Theoretical determination of the Co-C bond energy dissociation in cobalamins, *J. Am. Chem. Soc. 123*, 2679–2680.
51 Jensen, K. P., Ryde, U. (2002) The axial N-base has minor influence on Co-C bond cleavage in cobalamins, *J. Mol. Struct. (Theochem) 585*, 239–255.
52 Wetmore, S. D., Smith, D. M., Bennett, J. T., Radom, L. (2002) Understanding the mechanism of action of B_{12}-dependent ethanolamine ammonia-lyase: Synergistic interactions at play, *J. Am. Chem. Soc. 124*, 14054–14065.
53 Freindorf, M., Kozlowski, P. M. (2004) A combined density functional theory and molecular mechanics study of the relationship between the structure of coenzyme B_{12} and its binding to methylmalonyl-CoA mutase, *J. Am. Chem. Soc. 126*, 1928–1929.
54 Loferer, M. J., Webb, B. M., Grant, G. H., Liedl, K. R. (2003) Energetic and stereochemical effects of the protein environment on substrate: A theoretical study of methylmalonyl-CoA mutase, *J. Am. Chem. Soc. 125*, 1072–1078.
55 Jensen, K. P., Ryde, U. (2003) Theoretical prediction of the Co-C bond strength in cobalamins, *J. Phys. Chem. A107*, 7539–7545.
56 Doelker, N., Maseras, F., Siegbahn, P. E. M. (2004) Stabilization of the adenosyl radical in coenzyme B_{12} – a theoretical study, *Chem. Phys. Lett. 386*, 174–178.
57 Truhlar, D. G. Variational Transition State Theory and Multidimensional Tunneling for Simple and Complex Reactions in the Gas Phase, Solids, Liquids, and Enzymes, in *Isotope Effects in Chemistry and Biology*, H. Limbach, A. Kohen (Eds.), Dekker, New York, pp. 579–619.
58 Fernández-Ramos, A., Miller, J. A., Klippenstein, S. J., Truhlar, D. G. Modeling the Kinetics of Bimolecular Reactions, *Chem. Rev.* submitted for publication.
59 Truhlar, D. G., Gao, J., Garcia-Viloca, M., Alhambra, C.,

Corchado, J., Sanchez, L., Poulsen, T. D. (2004) Ensemble-averaged variational transition state theory with optimized multidimensional tunneling for enzyme kinetics and other condensed-phase reactions, *Int. J. Quantum Chem.*, *100*, 1136–1152.

60 Dybala-Defratyka, A., Paneth, P. (2001) Theoretical evaluation of the hydrogen kinetic isotope effect on the first step of the methylmalonyl-CoA mutase reaction, *J. Inorg. Biochem.* 86, 681–689.

61 Toraya, T., Yoshizawa, K., Eda, M., Yamabe, K. (1999) Direct participation of potassium ion in the catalysis of coenzyme B_{12}-dependent diol dehydratase, *J. Biochem.* (*Tokyo*) *126*, 650–654.

62 Toraya, T., Eda, M., Kamachi, T., Yoshizawa, K. (2001) Energetic feasibility of hydrogen abstraction and recombination in coenzyme B_{12}-dependent diol dehydratase reaction, *J. Biochem.* (*Tokyo*) *130*, 865–872.

63 Eda, M., Kamachi, T., Yoshizawa, K., Toraya, T. (2002) Theoretical study on the mechanism of catalysis of coenzyme B_{12}-dependent diol dehydratase, *Bull. Chem. Soc. Jpn.* *75*, 1469–1481.

64 Semialjac, M., Schwarz, H. (2004) Computational investigation of hydrogen abstraction from 2-aminoethanol by the 1,5-dideoxyribose-5-yl radical: A model study of a reaction occurring in the active site of ethanolamine ammonia lyase, *Chem.: Eur. J.* *10*, 2781–2788.

65 Dybala-Defratyka, A., Paneth, P., Pu, J., Truhlar, D. G. (2004) Benchmark results for hydrogen atom transfer between carbon centers and validation of electronic structure methods for bond energies and barrier heights, *J. Phys. Chem. A* *108*, 2475–2486.

66 Gao, J., Truhlar, D. G. (2002) Quantum mechanical methods for enzyme kinetics, *Annu. Rev. Phys. Chem.* *53*, 467–505.

67 Cramer, C. J. *Essentials of Computational Chemistry: Theories and Methods*, Wiley, Chichester, 2002.

68 Gonzàlez-Lafont, A., Truong, T. N., Truhlar, D. G. (1991) Direct dynamics calculations with neglect of diatomic differential overlap molecular orbital theory with specific reaction parameters, *J. Phys. Chem.* *95*, 4618–4627.

69 Lynch, B. J., Fast, P. L., Harris, M., Truhlar, D. G. (2000) Adiabatic connection for kinetics, *J. Phys. Chem. A* *104*, 4811–4815.

70 Eagar, R. G. Jr., Bachovchin, W. W., Richards, J. H. (1975) Mechanism of action of adenosylcobalamin: 3-Fluoro-1,2-propanediol as substrate for propanediol dehydratase-mechanistic implications, *Biochemistry* *14*, 5523–5528.

71 Dybala-Defratyka, A. (2004) Ph. D. Thesis, Technical University of Lodz, Poland; Dybala-Defratyka, A., Paneth, P., Truhlar, D. G., unpublished results.

72 Eyring, H. (1938) The theory of absolute reaction rates, *Trans. Faraday Soc.* *34*, 41–48.

73 Gonzàlez-Lafont, A., Truong, T. N., Truhlar, D. G. (1991) Interpolated variational transition state theory: Practical methods for estimating variational transition state properties and tunneling contributions to chemical reaction rates from electronic structure calculations, *J. Chem. Phys.* *95*, 8875–8894.

74 Truhlar, D. G., Kuppermann, A. (1971) Exact tunneling calculations, *J. Am. Chem. Soc.* *93*, 1840–1851.

75 Garrett, B. C., Truhlar, D. G., Grev, R. S., Magnuson, A. W. (1980) Improved treatment of threshold contributions in variational transition state theory, *J. Phys. Chem.* *84*, 1730–1748.

76 Marcus, R. A. (1966) On the analytical mechanics of chemical reactions. Quantum mechanics of linear collisions, *J. Chem. Phys.* *45*, 4493–4499.

77 Kuppermann, A., Adams, J. T., Truhlar, D. G. (1973) Streamlines of probability current density and

tunneling fractions for the collinear $H + H_2 \rightarrow H_2 + H$ reaction, in *Electronic and Atomic Collisions: Abstracts of Papers, Eighth International Conference on the Physics of Electronic and Atomic Collisions (VIII ICPEAC), Beograd, 1973*, B. C. Cobic, M. V. Kurepa (Eds.), Institute of Physics, Beograd, pp. 149–150.

78 Skodje, R. T., Truhlar, D. G., Garrett, B. C. (1982) Vibrationally adiabatic models for reactive tunneling, *J. Chem. Phys. 77*, 5955–5976.

79 Kreevoy, M. M., Ostovic, D., Truhlar, D. G., Garrett, B. C. (1986) Phenomenological manifestations of large-curvature tunneling in hydride transfer reactions, *J. Phys. Chem. 90*, 3766–3774.

80 Miller, W. H., Handy, N. C., Adams, J. E. (1980) Reaction path Hamiltonian for polyatomic molecules, *J. Chem. Phys. 72*, 99–112.

81 Truhlar, D. G., Isaacson, A. D., Garrett, B. C. (1985) Generalized transition state theory, in *Theory of Chemical Reaction Dynamics*, M. Baer (Ed.), CRC Press, Boca Raton, FL, Vol. 4, pp. 65–137.

82 Lu, D.-h., Truong, T. N., Melissas, V. S., Lynch, G. C., Liu, Y.-P., Garrett, B. C., Steckler, R., Isaacson, A. D., Rai, S. N., Hancock, G. C., Lauderdale, J. G., Joseph, T., Truhlar, D. G. (1992) POLYRATE 4: A new version of a computer program for the calculation of chemical reaction rates for polyatomics, *Comput. Phys. Commun. 71*, 235–262.

83 Liu, Y.-P., Lynch, G. C., Truong, T. N., Lu, D.-h., Truhlar, D. G., Garrett, B. C. (1993) Molecular modeling of the kinetic isotope effect for the [1,5]-sigmatropic rearrangement of *cis*-1,3-pentadiene, *J. Am. Chem. Soc. 115*, 2408–2415.

84 Marcus, R. A., Coltrin, M. E. (1977) A new tunneling path for reactions such as $H + H_2 \rightarrow H_2 + H$, *J. Chem. Phys. 67*, 2609–2613.

85 Schatz, G. C., Ratner, M. A. (1993) *Quantum Mechanics in Chemistry*, Prentice-Hall, Englewood Cliffs, NJ, pp. 167–181.

86 Garrett, B. C., Truhlar, D. G., Wagner, A. F., Dunning, T. H. Jr. (1983) Variational transition state theory and tunneling for a heavy-light-heavy reaction using an *ab initio* potential energy surface. $^{37}Cl + H(D)^{35}Cl \rightarrow H(D)^{37}Cl + {}^{35}Cl$, *J. Chem. Phys. 78*, 4400–4413.

87 Marcus, R. A. (1979) Similarities and differences between electron and proton transfers at electrodes and in solution. Theory of a hydrogen evolution reaction, in *Proceedings of the Third Symposium on Electrode Processes*, S. Bruckenstein, J. D. E. McIntyre, B. Miller, and E. Yeager (Eds.), Electrochemical Society, Princeton, pp. 1–12.

88 Chuang, Y.-Y., Corchado, J. C., Fast, P. L., Villà, J., Hu, W.-P., Liu, Y.-P., Lynch, G. C., Jackels, C. F., Nguyen, K. A., Gu, M. Z., Rossi, I., Coitiño, E. L., Clayton, S., Melissas, V. S., Lynch, B. J., Steckler, R. B., Garrett, C., Isaacson, A. D., Truhlar, D. G. (2000) POLYRATE–Version 8.4.1.PL, University of Minnesota, Minneapolis.

89 Garrett, B. C., Abusalbi, N., Kouri, D. J., Truhlar, D. G. (1983) Test of variational transition state theory and the least-action approximation for multidimensional tunneling probabilities against accurate quantal rate constants for a collinear reaction involving tunneling in an excited state, *J. Chem. Phys. 83*, 2252–2258.

90 Truong, T. N., Lu, D.-h., Lynch, G. C., Liu, Y.-P., Melissas, V. S., Stewart, J. J. P., Steckler, R., Garrett, B. C., Isaacson, A. D., González-Lafont, A., Rai, S. N., Hancock, G. C., Joseph, T., Truhlar, D. G. (1993) MORATE: A program for direct dynamics calculations of chemical reaction rates by semiempirical molecular orbital theory, *Comput. Phys. Commun. 75*, 143–159.

91 Liu, Y.-P., Lu, D.-h., González-Lafont, A., Truhlar, D. G., Garrett, B. C. (1993) Direct dynamics calculation of the kinetic isotope effect for an organic hydrogen-transfer

reaction, including corner-cutting tunneling in 21 dimensions, *J. Am. Chem. Soc. 115*, 7806–7817.

92 GARRETT, B. C., TRUHLAR, D. G. (1983) A least-action variational method for calculating multi-dimensional tunneling probabilities for chemical reactions, *J. Chem. Phys. 79*, 4931–4938.

93 ALLISON, T. C., TRUHLAR, D. G. Testing the accuracy of practical semiclassical methods: Variational transition state theory with optimized multidimensional tunneling, in *Modern Methods for Multidimensional Dynamics Computations in Chemistry*, D. L. THOMPSON (Ed.), World Scientific Singapore, 1998, pp. 618–712.

94 CHUANG, Y.-Y., FAST, P. L., HU, W.-P., LYNCH, G. C., LIU, Y.-P., TRUHLAR, D. G. (2001) MORATE-version 8.5, University of Minnesota, Minneapolis.

95 MASUDA, J., SHIBATA, N., MORIMOTO, Y., TORAYA, T., YASUOKA, N. (2000) How a protein generates a catalytic radical from coenzyme B_{12}: X-ray structure of a diol-dehydratase-adeninylpentylcobalamin complex, *Structure Fold. Des. 8*, 775–788.

96 GRUBER, K., REITZER, R., KRATKY, C. (2001) Radical shuttling in a protein: Ribose pseudorotation controls alkyl-radical transfer in the coenzyme B_{12} dependent enzyme glutamate mutase, *Angew. Chem. Int. Ed. Engl. 40*, 3377–3380.

97 LICHT, S., GERFEN, G. J., STUBBE, J. (1996) Thiyl radicals in ribonucleotide reductases, *Science 271*, 477–481.

98 BERTI, P. J., SCHRAMM, V. L. (1999) Enzymatic transition state structures constrained by experimental kinetic isotope effects: Experimental measurement of transition state variability, *ACS Symp. Ser. 721*, 473–488.

99 WARNCKE, K., SCHMIDT, J. C., KE, S.-C. (1999) Identification of a rearranged-substrate, product radical intermediate and the contribution of a product radical trap in vitamin B_{12} coenzyme-dependent ethanolamine deaminase catalysis, *J. Am. Chem. Soc. 121*, 10522–10528.

100 DOWD, P., TRIVEDI, B. K. (1985) On the mechanism of action of vitamin B_{12}. Model studies directed toward the hydrogen abstraction reaction, *J. Org. Chem. 80*, 206–217.

101 DOWD, P., WILK, B., WILK, B. K. (1992) First hydrogen abstraction-rearrangment modle for the coenyme B_{12}-dependent methylmalonyl-CoA to succinyl-CoA carbon skeleton rearranment reaction, *J. Am. Chem. Soc. 114*, 7949–7951.

102 DOLL, K. M., FINKE, R. G. (2003) A compelling experimental test of the hypothesis that enzymes have evolved To enhance quantum mechanical tunneling in hydrogen transfer reactions: The β-neopentylcobalamin system combined with prior adocobalamin data, *Inorg. Chem. 42*, 4849–4856.

103 DOLL, K. M., BENDER, B. R., FINKE, R. G. (2003) The first experimental test of the hypothesis that enzymes have evolved to enhance hydrogen tunneling, *J. Am. Chem. Soc. 125*, 10877–10884.

104 KEMSLEY, J. (2003) Enzyme tunneling idea questioned, *Chem. Eng. News 81*(38), 29–30.